Fluorescence Emission Anisotropy Coupled to an Electrochemical System: Study of Exciton Dynamics in Conjugated Polymers

ARTICLE *in* THE JOURNAL OF PHYSICAL CHEMISTRY C · DECEMBER 2007

Impact Factor: 4.77 · DOI: 10.1021/Jp075587j

4 AUTHORS:

Francisco Montilla
University of Alicante
53 PUBLICATIONS **1,016** CITATIONS
SEE PROFILE

Luis Manuel Frutos
University of Alcalá
56 PUBLICATIONS **924** CITATIONS
SEE PROFILE

C.Reyes Mateo
Universidad Miguel Hernández de Elche
58 PUBLICATIONS **1,217** CITATIONS
SEE PROFILE

Ricardo Mallavia
Universidad Miguel Hernández de Elche
102 PUBLICATIONS **1,251** CITATIONS
SEE PROFILE

Fluorescence Emission Anisotropy Coupled to an Electrochemical System: Study of Exciton Dynamics in Conjugated Polymers

F. Montilla,*,† L. M. Frutos,‡ C. R. Mateo,§ and R. Mallavia§

Instituto Universitario de Materiales de Alicante and Departamento de Química Física, Universidad de Alicante, Apartado de Correos 99, Alicante, Spain E-03080, Institute of Physical and Theoretical Chemistry, Technical University of Munich, D-85747 Garching, Germany, and Instituto de Biología Molecular y Celular, Universidad Miguel Hernández, Avenida de la Universidad s/n, Elche (Alicante), Spain E-03202

Received: July 17, 2007; In Final Form: September 17, 2007

Emission anisotropy studies have been performed for two types of conjugated polymers: phenylene−vinylene (MDMO−PPV) and fluorene−phenylene (PFP) based polymers. The emission from polymer films deposited onto ITO plates is strongly depolarized due to resonance energy homotransfer in both polymers. This transfer is more efficient for MDMO−PPV than for PFP. The anisotropy of both polymers rises during electrochemical doping. The introduction of randomly distributed quenchers in the conjugated polymer chains decreases the exciton lifetime and therefore the mean free path of each exciton, producing the increase of anisotropy. In addition, green emission bands coming from degraded polyfluorenes have been analyzed by in situ electrochemical polarized fluorescence. The emission from extensively thermal-oxidized polyfluorene is depolarized by exciton transfer between defective fluorenone sites with different orientation of the transition dipole. Conversely, the green emission from electrochemically degraded PFP shows a high polarization degree, suggesting the presence of ordered domains.

1. Introduction

Exciton dynamics are of great importance for the application of conjugated polymers to light-emitting or photovoltaic devices.[1−4] On the one hand, the efficiency of emitting diodes decreases by exciton migration to the cathode or to interchain quenching sites. On the other hand, high diffusion lengths are required for photovoltaic application, where the exciton must move to an interphase site for an effective charge separation.

In light-emitting materials an excited state can undergo radiative or nonradiative relaxation processes and can transfer its electronic energy to another chromophore.[5] In disordered molecular materials, such as conjugated polymers in solid phase, the Förster model has been applied to predict energy transfer between two chromophores by dipole−dipole interactions. Due to the energy transfer from the initially excited chromophore to a randomly oriented neighbor, the steady-state fluorescence emission of conjugated polymers in solid phase presents a high isotropic character.[6,7]

Polarized fluorescence experiments have been usually applied to the study of anisotropic polymer samples including liquid crystal, photoaddressed polymers, and chirally organized layers, etc.[8−11] These systems find application in the fabrication of polarized light-emitting devices.[12]

Time-resolved fluorescence spectroscopy has been used for the determination of the exciton motion in a conjugated PPV[4,13]- or conjugated perylene derivative chromophores.[14] Fluorescence anisotropy in these solid-state systems decays to low values at room temperature indicating depolarization mainly due to intermolecular exciton diffusion.[6,7,14]

Fluorene-based conjugated polymers (PF) have been extensively studied for their emissive properties. The excitation migration of this type of polymer was studied by Vaughan et al. making use of fluorescence anisotropy.[15] The exciton migration along the conjugated polymer chains in solution involves conformational relaxation by twisting of part of the chain within 20 or more repeat units.

Great attention has been paid to the degradation process of PF for its applications in blue-emitting diodes. The formation of green or g-bands upon degradation may appear by thermal, photochemical, or electrical-activated oxidation in the presence of oxygen. The growth of this band has been related to the formation of fluorenone defects.[16,17] However, the degradation mechanism is still under discussion. Zhao et al. have studied the role of cross-linked products formed by thermal oxidation,[18] while Sims et al. proposed the formation of fluorenone-based excimers.[37] The growth of the green band in PF-based light-emitting diodes was correlated by Lu et al. to the formation of fluorene-based excimers induced by an electric field and assisted by the motion of the side chain, although fluorenone defects were also formed upon diode fabrication.[19] Moreover, the growth of g-bands coming from the electrochemical degradation of polyfluorenes in the absence of oxygen have been related to the formation of cross-linked products.[20] The g-band obtained by electrochemical method is similar to those obtained in light-emitting devices operated in the absence of oxygen.[21−23]

This work combines the electrochemical control of a solid/liquid interface with the measurement of photoluminescence (in situ electrochemical fluorescence) for the study of the changes in the emission anisotropy of conjugated PF and phenylene−vinylene (MDMO−PPV) light-emitting polymers upon reversible electrochemical charge injection or doping. Special attention has been paid to the evolution of polarized emission in degraded

* To whom correspondence should be addressed. E-mail: francisco.montilla@ua.es.
† Universidad de Alicante.
‡ Technical University of Munich.
§ Universidad Miguel Hernández.

10.1021/jp075587j CCC: $37.00
Published on Web 11/17/2007

polyfluorenes, with a comparison of the polarization of the g-bands formed.

2. Experimental Section

Polymers. Poly[9,9-bis(6′-bromohexylfluoren-2,7-diyl)-alt-*co*-(benzen-1,4-diyl)] (PFP) has been synthesized via Suzuki coupling reaction using 1,4-phenyldiboronic acid and 2,7-dibromo-9,9-bis(6′-bromohexyl)fluorene as starting materials.[24] Poly-[2-methoxy-5-(3′,7′-dimethyloctyloxy)-1,4-phenylene-vinylene] (MDMO−PPV) was purchased from Aldrich. A 10 μL aliquot of a solution of polymer (1 mg/mL tetrahydrofuran (THF)) were spread over 1 cm^2 of ITO conductive glass (60 Ω^{-1} cm^{-1}).

Electro- and Spectro-electrochemical Measurements. The solvent for electrochemical measurements was acetonitrile (Merck, HPLC grade), and tetrabutylammonium tetrafluoroborate (Aldrich 99%) was used as supporting electrolyte. A platinum wire was used as auxiliary electrode. The reference electrode was an Ag/AgCl electrode (3 M KCl, Crison) for the conventional electrochemical cell and a silver wire as pseudo-reference electrode for the spectro-electrochemical cell, immersed in the same electrolytic solution. Spectro-electrochemical measurements (in situ electrochemical fluorescence) were performed in a modified fluorescence cell (1 cm length quartz cell). Details on the cell design were shown in a previous paper.[25]

The working electrode was a transparent ITO-glass electrode covered with conjugated polymer. The oxygen was purged from the electrochemical cells by bubbling argon for 20 min, and the argon atmosphere was maintained during all the experiments. To remove the water from the electrolytic solution, molecular sieve (4 Å, Scharlau) was placed into the cell. Fluorescence spectra and steady-state anisotropy measurements were performed at room temperature using a PTI QuantaMaster Model QM-62003SE spectrofluorometer. All the spectroelectrochemical experiments were reproduced at least two times.

3. Background for Polarized Fluorescence Measurements

For the steady-state anisotropy determination, the corresponding vertically polarized and horizontally polarized emission intensities elicited by vertically polarized excitation (I_{VV} and I_{VH}, respectively) were determined. The degree of polarization or anisotropy (r) of the polymer films can be calculated from

$$r = \frac{I_{VV} - GI_{VH}}{I_{VV} + 2GI_{VH}} \tag{1}$$

G is a correction factor related with the experimental setup. The G-factor, accounting for differential polarization sensitivity, was determined by measuring the polarized components of fluorescence of the sample with horizontally polarized excitation and can be calculated from

$$G = \frac{I_{HV}}{I_{HH}} \tag{2}$$

Photoselection with linearly polarized light leads to an anisotropic distribution of the transition moments of the excited molecules; therefore emitted light is polarized as well. The maximum theoretical anisotropy (or fundamental anisotropy, r_0) can be calculated from[26]

$$r_0 = \frac{2}{5}\left(\frac{3\cos^2\alpha - 1}{2}\right) \tag{3}$$

α being the angle between the absorption and emission transition moments. To give insight into the excitation and emission (fluorescence) of the chromophores present in the polymer, we have investigated theoretically these processes by using single-excitation configuration interaction method with a 6-31G(d) basis set as implemented in the Gaussian03 suite of programs (see Supporting Information). Concretely, we have studied the electronic and structural properties of the monomers in the ground and excited states in order to determine r_0 in different conditions. Since torsional modes are impeded by the experimental conditions (solid matrix), we have determined the fundamental anisotropy when stretching and/or full vibrational relaxation is taken into account. We find that a high fluorescence fundamental anisotropy characterizes both chromophores, and only some small deviation from the maximum anisotropy (i.e., $r_0 = 0.4$) is present when we take into account vibrational relaxation in the excited state.

However the emitted light is partially or completely depolarized by several causes, such as rotational diffusion of fluorophores or resonance energy transfer (RET). In the case of homotransfer (RET occurring between chemically identical molecules) and isotropic rotations, fluorescence anisotropy can be written as[27]

$$r = r_0 W_R W_T \tag{4}$$

with $W_i \leq 1$. W_R is a depolarization factor due to thermal rotations, and W_T is a depolarization factor related to RET. In samples with highly hindered rotational motion (i.e., frozen solutions or polymeric layers) the depolarization is only attributed to RET ($W_R = 1$). The rate constant for transfer between a donor and an acceptor at a distance R, following the Förster mechanism, is[26]

$$k_T = \frac{1}{\tau_D^0}\left[\frac{R_0}{R}\right]^6 \tag{5}$$

where τ_D^0 is the excited-state lifetime in the absence of transfer and R_0 is the Förster critical radius, that is, the distance at which transfer and spontaneous decay of the excited molecule is equally probable. R_0 is proportional to the fluorescent quantum yield (Q_D) and the spectral overlap (J) among other parameters:

$$R_0 = 0.211[Q_D \kappa^2 n^{-4} J]^{1/6} \tag{6}$$

κ^2 being the orientation factor and n the refractive index, with R_0 in Å and the spectral overlap in M^{-1} cm^{-1} nm^4 units.[27]

4. Results and Discussion

4.1. Optical and Electrochemical Characterization of the Polymers. Figure 1 shows the fluorescence and absorption spectra for PFP and MDMO−PPV deposited onto a quartz plate. PFP exhibits an absorption maximum at 372 nm, corresponding to the $\pi\pi^*$ transition of the polymer backbone. The emission maximum appears at 417 nm with a well-defined vibronic feature at 438 nm. MDMO−PPV has an absorption maximum at 472 nm with a bandwidth wider than PFP. Its emission spectrum is characterized by a maximum at 570 nm with a poorly defined vibronic feature around 610 nm.

The Förster critical radius calculated from eq 6 is $R_0 = 3$ nm for both polymers. Details on the calculation of R_0 and determination of spectral overlap and quantum yields can be found in the Supporting Information.

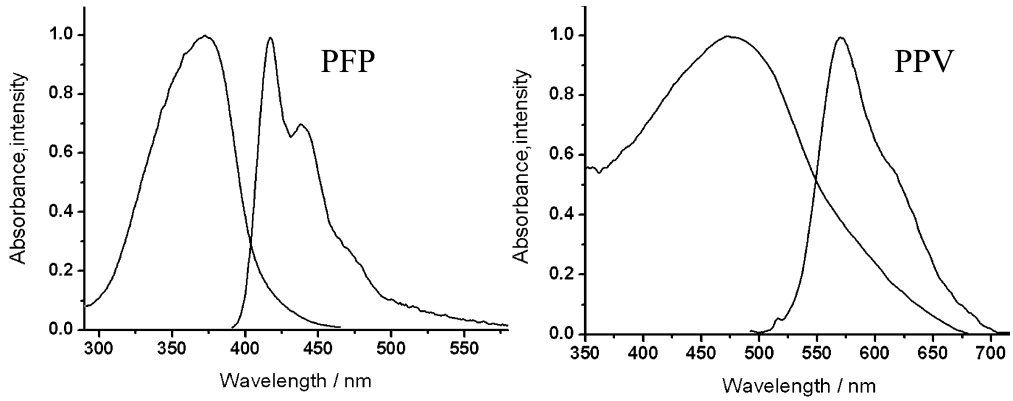

Figure 1. Normalized absorption and emission spectra for PFP (λ_{ex} = 370 nm) and MDMO−PPV (λ_{ex} = 467 nm) polymers supported onto quartz plates.

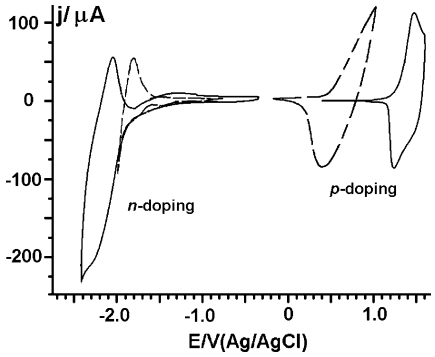

Figure 2. Cyclic voltammograms for PFP (solid lines) and MDMO−PPV (dashed lines) polymers supported onto ITO plates. Scan rate, 100 mV s^{-1}.

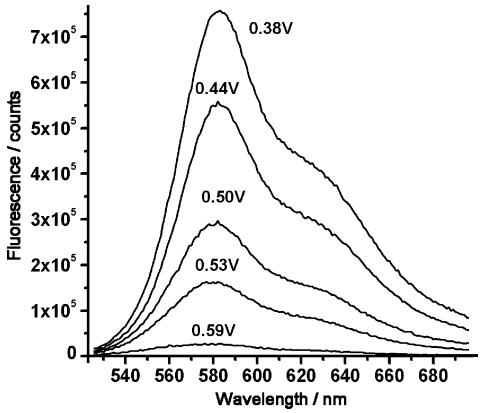

Figure 3. Evolution of the fluorescence spectra as function of the potential during the electrochemical doping of a MDMO−PPV polymer deposited onto an ITO plate (λ_{ex}= 467 nm).

Figure 2 shows the stabilized voltammograms of the reversible doping processes for both PFP and MDMO−PPV polymers.

The p-doping process of both polymers appears in the right part of the figure. In the positive-going scan, an oxidation current emerges around +0.4 V for MDMO−PPV, while the oxidation onset for PFP is around +1.1 V. The oxidation onset is a direct measure of the energetic position of HOMO level (−4.8 eV for MDMO−PPV and −5.5 eV for PFP). The oxidation process is reversible for both polymers. The voltammetric scan is reverted at +1.0 V for MDMO−PPV and the corresponding reduction peak appearing at +0.4 V, indicative of the dedoping of the polymer. A similar process appears for PFP when the voltammetric scan is reverted at +1.6 V; the reduction peak centered at +1.2 V is related to the polymer dedoping.

The left side of Figure 2 shows the voltammetric features related to n-doping. In the scan to less positive potentials, a negative current emerges at −1.6 V for MDMO−PPV. The reduction onset appears at −1.7 V for PFP. From these potentials the value of LUMO levels for both polymers were established (−2.8 eV for MDMO−PPV and −2.7 eV for PFP). These processes are also reversible, and the dedoping of the polymers is observed during the reverse scan.

4.2. Spectroelectrochemistry of the Polymers. A series of fluorescence spectra were collected upon electrochemical doping of MDMO−PPV. Figure 3 shows the evolution of the emission spectrum upon electrochemical p-doping. The fluorescence spectrum remains unmodified before polymer oxidation. When the potential is stepped to values more-positive than +0.4 V, the fluorescence intensity starts to drop. The fluorescence is completely quenched at +0.65 V. This is a reversible process for potentials up to +1.0 V, and therefore the fluorescence can be recovered upon dedoping.[28] At more-positive potentials the polymer suffers degradation and the fluorescence cannot be restored by electrochemical reduction.

The fluorescence can be also reversibly quenched during the reduction of the MDMO−PPV polymer at potentials between −1.6 and −1.9 V. The application of potentials less-positive than −1.9 produces the complete and irreversible deactivation of the emission of this polymer.

Detailed studies on the electrochemical quenching of PFP polymers have been presented in previous papers.[20,25] In a manner similar to that of MDMO−PPV, fluorescent emission of PFP can be reversibly quenched by oxidation at potentials between +1.1 and +1.6 V.

Upon electrochemical n-doping, fluorescence is quenched reversibly between −1.7 and −2.2 V. At potentials less-positive than −2.2 V the emission band centered at 420 nm is not completely quenched. A new emission band appears centered at 490 nm upon irreversible reduction (see section 4.4).[20]

4.3. Polarized Fluorescence of Polymers. The steady-sate polarized spectra for MDMO−PPV and PFP polymers deposited onto an ITO plate are shown in Figure 4, and the fluorescence anisotropy has been calculated as a function of the emission wavelength.

The emission anisotropy is low for both polymers (r = 0.08 at 422 nm for PFP and r = 0.02 at 590 nm for MDMO−PPV), indicating that the fluorescence is highly depolarised. The depolarization is more efficient for MDMO−PPV than for PFP.

Considering the polymer layer as an isotropic material of randomly oriented chromophores and unable to rotate, the Förster resonance energy transfer between chromophores serves to randomize the orientational distribution of the excited

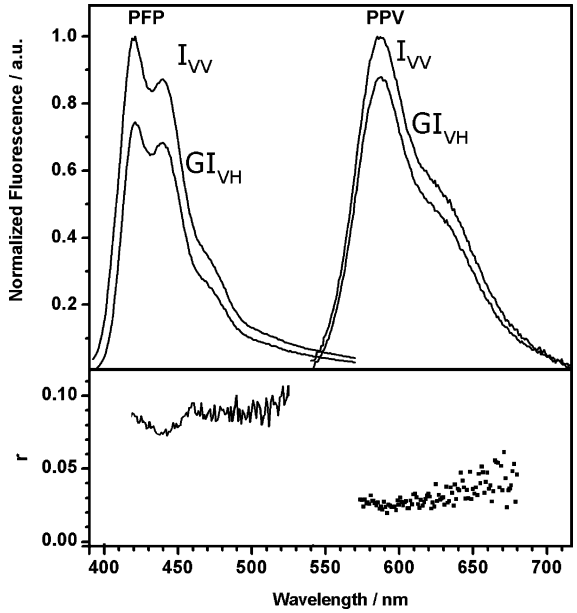

Figure 4. Top: Polarized emission for PFP (λ_{ex} = 370 nm) and MDMO−PPV (λ_{ex} = 467 nm) deposited onto ITO plates. Bottom: Emission anisotropy (*r*) for PFP and MDMO−PPV deposited onto ITO plates. The horizontally polarized emission was corrected with the *G*-factor of the eq 2.

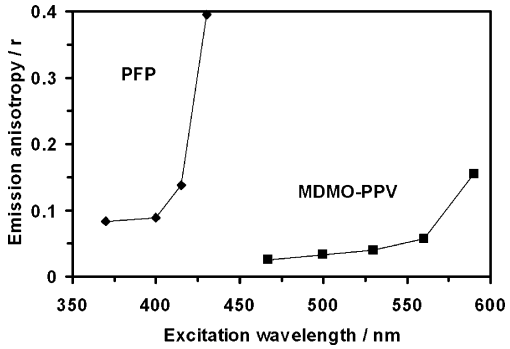

Figure 5. Fluorescence emission anisotropy of PFP and MDMO−PPV as a function of the excitation wavelength.

molecules. When the anisotropy of the polymer is measured by exciting in the red-edge of the absorption spectrum, an increase of the anisotropy is observed in Figure 5. The lack of energy transfer (Weber's or red-edge effects[29]) upon red-edge excitation confirms the cause of the depolarization.

Since the value of the Förster critical radius is very similar for both polymers, the higher depolarization factor in MDMO−PPV than in PFP must be related to a higher efficiency of the energy-transfer process in the former polymer, which could be due to a higher diffusion coefficient of the exciton in MDMO−PPV.

The evolution of the emission anisotropy upon electrochemical treatment has been measured in the following experiments. Figure 6 shows the evolution of the anisotropy in the emission maxima during the electrochemical doping of the polymers. During the oxidation or p-doping of MDMO−PPV (Figure 6b, right) an increase of the anisotropy from 0.02 to 0.22 can be observed at +0.7 V.

A similar increase of *r* is observed during the electrochemical reduction (n-doping, Figure 6b, left side) of the polymer. The maximum value of anisotropy is now around 0.09 at the highest values of doping. The differences between the maximum value reached is related to the lower quenching efficiency of electrons with respect to holes.[30]

This result may indicate that the best performances in polarized light-emitting diodes, in terms of polarization ratio, must appear when the device has a high concentration of charge carriers during operation. A high concentration of holes or electrons in the device promotes the quenching of the excitons by the electrogenerated charge carriers and must therefore improve the polarization ratio of such devices. Several authors have pointed out the improvement of the performance of polarized light-emitting diodes by the use of charge transporting molecules on diode preparation such as hole transporting photoalignment polymers[31,32] or electron conducting layers.[33] These components added to the devices improve the external efficiency or luminance of the diodes. The present work suggests that the polarization ratio is also enhanced by the charge carrier properties of the emitting layer. Furthermore, the polarization ratio of the devices would rise as a function of the applied external potential, since the concentration of the charge carrier is proportional to the applied bias potential. This result explains the much higher polarization ratio observed in electroluminescent devices compared with the equivalent devices in photoluminescence.[34,35]

The behavior of PFP upon doping by positive charges is shown in Figure 6a (right side). The initial anisotropy value remains constant up to potentials less-positive than +1.1 V. The anisotropy rises upon p-doping, reaching a value of *r* around 0.2 at +1.45 V, indicating the lowering of RET by quenching of the exciton.

A phenomenological approach can give some information about the dynamics of the excited state in these polymers. The injection of polarons in the conjugated chain induces the quenching of the fluorescence.[25] The injection of charge produces the decrease of the lifetime of the excited state, and therefore decreases the probability of the exciton migration to neighbor chains. The rise of the anisotropy can be related to the decreased mean free path of the photogenerated excitons that is proportional to the presence of randomly distributed quenchers during doping of the polymeric layer. An effective correlation time for the energy-transfer depolarization could be determined assuming a monoexponential emission anisotropy decay. The effective correlation time calculated from the steady-state anisotropy values at different potentials for PFP is longer than for PPV, indicating that the diffusion coefficient of the excitons in the former polymer is lower than in PPV. However to extract meaningful information from these steady-state measurements, it is necessary to perform further time-resolved experiments.

The evolution of the anisotropy during reduction of the polymer is quite different. At initial stages of the n-doping (between −1.3 and −2.2 V; left side of Figure 6a), the anisotropy rises as expected, but when the applied potential is less-positive than −2.2 V a sudden decrease of the anisotropy at 420 nm is observed. At these potentials a highly depolarized blue emission is observed. This behavior is related to the growth of a green-emitting band upon electrochemical reduction at those potentials. In the following section we have focused our attention in the study of the polarization of the light coming from green-emitting products in degraded polyfluorenes.

4.4. Polarized Fluorescence of Green-Emitting Bands of Polyfluorenes. Figure 7 shows the unpolarized fluorescence spectra of degraded PFP. Thermal degradation (Figure 7a) was performed by heating ITO/polymer plates at 200 °C under air flow for different times. A growing green band can be observed at 535 nm, coming mainly from fluorenone defects formed upon oxidation[16] and with some contributions of cross-linked poly-

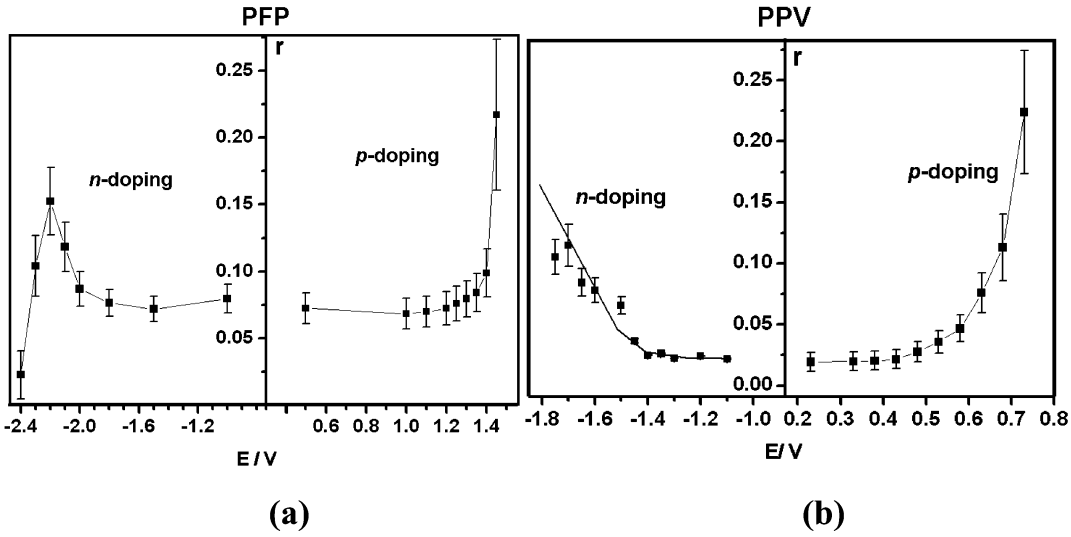

Figure 6. Evolution of the fluorescence anisotropy of **(a)** PFP (λ_{ex} = 370 nm, λ_{em} = 420 nm) and **(b)** MDMO−PPV (λ_{ex} = 467 nm, λ_{em} = 570 nm) as a function of the potential during the electrochemical doping of the polymers.

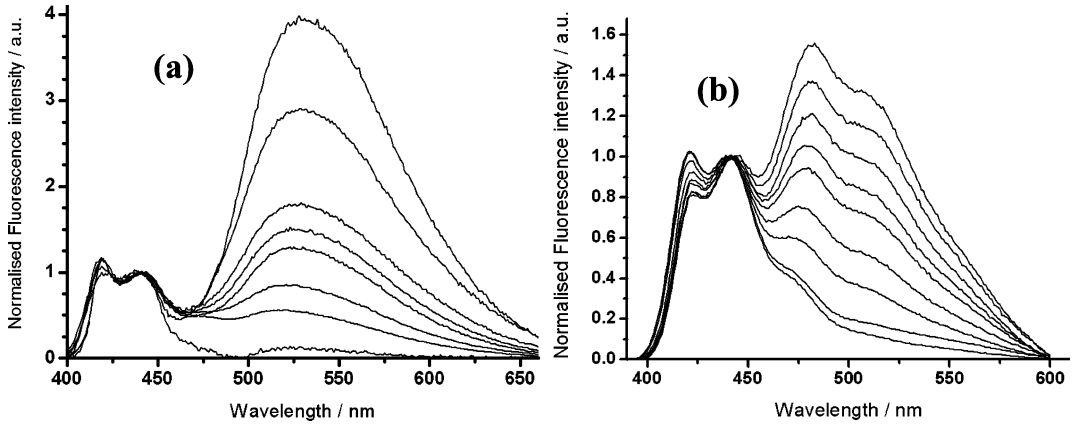

Figure 7. Fluorescence spectra of degraded PFP (λ_{ex} = 370 nm). The spectra were normalized in the vibronic maximum at 438 nm. (a) Thermally degraded ITO/PFP plates at 200 °C under air. (b) Electrochemically degraded ITO/PFP by reduction at −2.2 V.

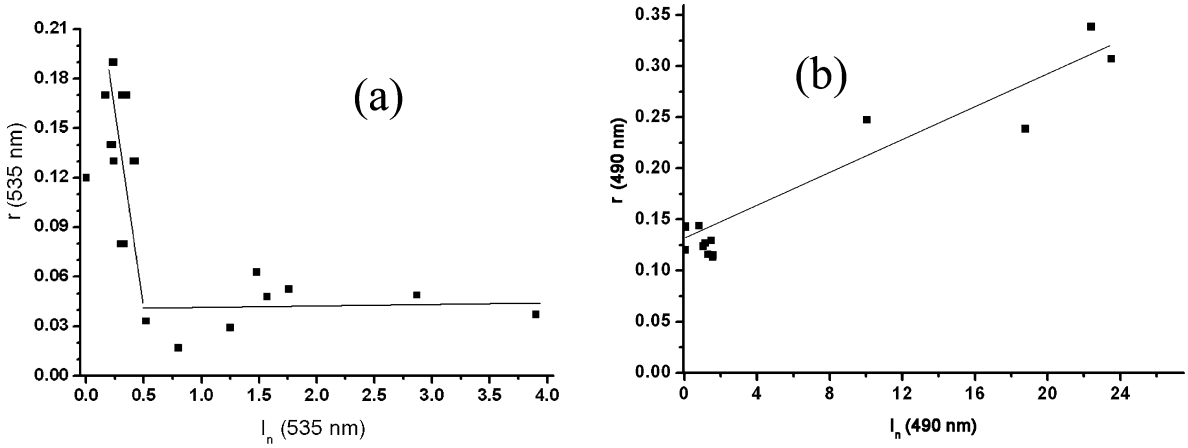

Figure 8. Fluorescence anisotropy of degraded PFP as a function of the fluorescence intensity of g-bands. (a) Thermally degraded PFP (λ_{ex} = 370 nm, λ_{em} = 535 nm). (b) Electrochemically degraded PFP (λ_{ex} = 370 nm, λ_{em} = 490 nm).

mer.[18] Figure 7b shows the spectra for PFP electrochemically reduced at −2.2 V. The growing green emission band at 485 nm has been related to cross-linked polymer formed upon electrochemical reduction.[20]

A study of the variation of the fluorescence anisotropy as a function of the degree of the degradation of PFP was performed. Figure 8a shows the value of anisotropy at 535 nm for thermally degraded PFP as a function of the intensity of the green band. The intensity of this band is related to the amount of fluorenone defects.[36] When the amount of defects is low, the anisotropy remains high, indicating that the excited state of the photoselected fluorenones remain trapped in these low-energy defects and little RET happens to neighbors.[8]

Low values of anisotropy appear when the amount of defects increases, indicating that the exciton in the photoselected fluorenones are able to transfer energy to a site with similar energy (another fluorenone site) but different dipole orientation. This is indicative of the presence of fluorenone defects near

the photoselected fluorenone and an effective Forster energy transfer may happen between dipoles with similar energies.

The situation is quite different for the electro-degraded polymer. When the amount of green-emitting product formed by reduction is low, there are no significant changes in the value of anisotropy. As shown in Figure 8b for high intensity of the g-band an increase of the anisotropy can be observed to values around 0.25−0.35. The high polarization of the emission may be related to the formation of ordered domains that have been induced upon electrochemical degradation. We previously proposed the formation of excimeric species by electrochemical cross-linking reactions.[20] The evolution of the anisotropy is in good agreement with the hypothesis of the formation of highly ordered domains (π-stacked) in the polymeric matrix by the electrochemical treatment. The energy transfer of these low-energy excitons is effective within these ordered domains, characterized by the same orientation of dipoles between adjacent molecules, producing therefore a high value of anisotropy.

5. Conclusions

Fluorescence emission anisotropy coupled to an electrochemical system is a powerful tool for the study of exciton dynamics in conjugated polymers. The fundamental anisotropy has been determined by calculation of the angles formed by the dipole moments of the monomers in its ground and excited state. In solid state the experimentally measured anisotropy of the polymers is much lower than the limiting anisotropy. The depolarization of the emission is due to resonance energy homotransfer.

The injection of charge in the polymeric layer by electrochemical methods produces the increase of the anisotropy. This effect is due to the decreasing of the exciton lifetime upon quenching by polarons, and therefore lowering of the efficiency of homotransfer. The injection of holes induces a higher polarization of the emission compared with electrons.

The study of polarized emission in degraded polyfluorenes confirms the different nature of the green emission bands obtained by thermal and electrochemical degradation. While the g-bands in thermally degraded PFP are depolarized by RET between low-energy defective sites, the green emission from electrochemically degraded samples is highly polarized. This result is indicative of the presence of ordered domains formed by electrochemical reduction.

Acknowledgment. This work is financed by Project MAT-2005-1004 of the Spanish Ministerio de Educación y Ciencia. F.M. and R.M. acknowledge the financial support given by "Ramón y Cajal" programs. L.M.F acknowledges the "Alexander von Humboldt" Foundation for a postdoctoral grant.

Supporting Information Available: Calculations of the transition dipole moments for the monomeric species and the determination of spectral overlap, quantum yields, and Förster critical radius for both polymers. This material is available free of charge via the Internet at http://pubs.acs.org.

References and Notes

(1) Chen, P.; Yang, G. Z.; Liu, T. X.; Li, T. C.; Wang, M.; Huang, W. *Polym. Int.* **2006**, *55* (5), 473−490.

(2) Bredas, J. L.; Beljonne, D.; Coropceanu, V.; Cornil, J. *Chem. Rev.* **2004**, *104*, 4971−5003.

(3) Ruseckas, A.; Wood, P.; Samuel, I. D. W.; Webster, G. R.; Mitchell, W. J.; Burn, P. L.; Sundstrom, V. *Phys. Rev. B* **2005**, *72* (11), 115214.

(4) Markov, D. E.; Blom, P. W. M. *Phys. Rev. B* **2006**, *74* (8), 085206.

(5) Stork, M.; Gaylord, B. S.; Heeger, A. J.; Bazan, G. C. *Adv. Mater.* **2002**, *14* (5), 361−366.

(6) Gaab, K. M.; Bardeen, C. J. *J. Phys. Chem. A* **2004**, *108*, 10801−10806.

(7) Gaab, K. M.; Bardeen, C. J. *J. Phys. Chem. B* **2004**, *108*, 4619−4626.

(8) Yang, X. H.; Neher, D.; Spitz, C.; Zojer, E.; Bredas, J. L.; Guntner, R.; Scherf, U. *J. Chem. Phys.* **2003**, *119* (13), 6832−6839.

(9) Fritz, K. P.; Scholes, G. D. *J. Phys. Chem. B* **2003**, *107*, 10141−10147.

(10) Palsson, L. O.; Vaughan, H. L.; Monkman, A. P. *J. Chem. Phys.* **2006**, *125* (16), 164701.

(11) Molina, R.; Ramos, M.; Montilla, F.; Mateo, C. R.; Mallavia, R. *Macromolecules* **2007**, *40*, 3042−3048.

(12) Satrijo, A.; Meskers, S. C. J.; Swager, T. M. *J. Am. Chem. Soc.* **2006**, *128*, 9030−9031.

(13) Bjorklund, T. G.; Lim, S. H.; Bardeen, C. J. *J. Phys. Chem. B* **2001**, *105*, 11970−11977.

(14) Al-Kaysi, R. O.; Ahn, T. S.; Muller, A. M.; Bardeen, C. J. *Phys. Chem. Chem. Phys.* **2006**, *8* (29), 3453−3459.

(15) Vaughan, H. L.; Dias, F. M. B.; Monkman, A. P. *J. Chem. Phys.* **2005**, *122* (1), 14902.

(16) Gamerith, S.; Gadermaier, C.; Scherf, U.; List, E. J. W. *Phys. Status Solidi A* **2004**, *201* (6), 1132−1151.

(17) Grisorio, R.; Suranna, G. P.; Mastrorilli, P.; Nobile, C. F. *Adv. Funct. Mater.* **2007**, *17* (4), 538−548.

(18) Zhao, W.; Cao, T.; White, J. M. *Adv. Funct. Mater.* **2004**, *14* (8), 783−790.

(19) Lu, H. H.; Liu, C. Y.; Jen, T. H.; Liao, J. L.; Tseng, H. E.; Huang, C. W.; Hung, M. C.; Chen, S. A. *Macromolecules* **2005**, *38*, 10829−10835.

(20) Montilla, F.; Mallavia, R. *Adv. Funct. Mater.* **2007**, *17* (1), 71−78.

(21) Ouisse, T.; Stephan, O.; Armand, M. *Eur. Phys. J.: Appl. Phys.* **2003**, *24* (3), 195−200.

(22) Gong, X. O.; Iyer, P. K.; Moses, D.; Bazan, G. C.; Heeger, A. J.; Xiao, S. S. *Adv. Funct. Mater.* **2003**, *13* (4), 325−330.

(23) Gamerith, S.; Nothofer, H. G.; Scherf, U.; List, E. J. W. *Jpn. J. Appl. Phys., Part 2* **2004**, *43* (7 A), L891−L893.

(24) Mallavia, R.; Montilla, F.; Pastor, I.; Velasquez, P.; Arredondo, B.; Alvarez, A. L.; Mateo, C. R. *Macromolecules* **2005**, *38*, 3185−3192.

(25) Montilla, F.; Pastor, I.; Mateo, C. R.; Morallon, E.; Mallavia, R. *J. Phys. Chem. B* **2006**, *110*, 5914−5919.

(26) Valeur, B. *Molecular Fluorescence. Principles and Applications*; Wiley-VCH Verlag GmbH: Weinheim, Germany, 2001.

(27) Wieb Van Der Meer, B.; Coker, G.; Simon Chen, S.-Y. *Resonance Energy Transfer. Theory and Data*; VCH: Weinheim, Germany, 1994.

(28) Montilla, F.; Mallavia, R. *J. Phys. Chem. B* **2006**, *110*, 25791−25796.

(29) Demchenko, A. P. *Luminescence* **2002**, *17* (1), 19−42.

(30) Young, R. H.; Tang, C. W.; Marchetti, A. P. *Appl. Phys. Lett.* **2002**, *80* (5), 874−876.

(31) Aldred, M. P.; Vlachos, P.; Contoret, A. E. A.; Farrar, S. R.; Chung-Tsoi, W.; Mansoor, B.; Woon, K. L.; Hudson, R.; Kelly, S. M.; O'Neill, M. *J. Mater. Chem.* **2005**, *15* (31), 3208−3213.

(32) Grell, M.; Knoll, W.; Lupo, D.; Meisel, A.; Miteva, T.; Neher, D.; Nothofer, H. G.; Scherf, U.; Yasuda, A. *Adv. Mater.* **1999**, *11* (8), 671−675.

(33) Contoret, A. E. A.; Farrar, S. R.; Jackson, P. O.; Khan, S. M.; May, L.; O'Neill, M.; Nicholls, J. E.; Kelly, S. M.; Richards, G. J. *Adv. Mater.* **2000**, *12* (13), 971−974.

(34) Whitehead, K. S.; Grell, M.; Bradley, D. D. C.; Jandke, M.; Strohriegl, P. *Appl. Phys. Lett.* **2000**, *76* (20), 2946−2948.

(35) Neher, D. *Macromol. Rapid Commun.* **2001**, *22* (17), 1366−1385.

(36) Kulkarni, A. P.; Kong, X. X.; Jenekhe, S. A. *J. Phys. Chem. B* **2004**, *108*, 8689−8701.

(37) Sims, M.; Bradley, D. D. C.; Ariu, M.; Koeberg, M.; Asimakis, A.; Grell, M.; Lidzey, D. G. *Adv. Funct. Mater.* **2004**, *14* (8), 765−781.